Gating Orbital Memory with an Atomic Donor

Elze J. Knol, Brian Kiraly, Alexander N. Rudenko⬤, Werner M. J. van Weerdenburg⬤,
Mikhail I. Katsnelson⬤, and Alexander A. Khajetoorians⬤

Institute for Molecules and Materials, Radboud University, Nijmegen 6525AJ, Netherlands

Orbital memory is defined by two stable valencies that can be electrically switched and read out. To explore the influence of an electric field on orbital memory, we studied the distance-dependent influence of an atomic Cu donor on the state favorability of an individual Co atom on black phosphorus. Using low temperature scanning tunneling microscopy and spectroscopy, we characterized the electronic properties of individual Cu donors, corroborating this behavior with *ab initio* calculations based on density functional theory. We studied the influence of an individual donor on the charging energy and stochastic behavior of an individual Co atom. We found a strong impact on the state favorability in the stochastic limit. These findings provide quantitative information about the influence of local electric fields on atomic orbital memory.

A single magnetic atom on a surface can exhibit multiple valencies, as predicted for various $3d$ transition metal atoms on the surface of graphene [1,2]. This concept was experimentally demonstrated, using scanning tunneling microscopy and spectroscopy (STM/STS), with individual Co atoms on the surface of semiconducting black phosphorus (BP) [3]. In this study, the two stable valencies of an individual Co atom residing in a hollow site were observed via their different charge densities, and could be switched electrically, serving as a so-called orbital memory. Moreover, the electric field generated by the probe could be used to ionize an individual Co atom, leading to stochastic fluctuations between the stable configurations characterized by telegraph noise in the tunneling current. It was later shown that the stochastic behavior of arrays of coupled orbital memories exhibits tunable multiplicity, a precursor to glassy dynamics characteristic in multiwell systems [4–6]. In this way, arrays of orbital memories are a promising platform to mimic machine learning at the atomic scale, due to their long-range connectivity and competing interactions.

Understanding the influence of an electric field on orbital memory is vital both fundamentally as well as for its utility, in analogy to the effect of a magnetic field on spin-based memory [7–9]. One way to quantify the role of an electric field on the bistable valency is to place well-defined atomic-scale dopants near individual orbital memories and probe the response of the bistable valency. In this vain, it has been shown that alkali atoms are charge donors on the surface of BP. For instance, it was shown that K atoms can be used to *n*-dope BP [10–12] and probe the anisotropic dielectric screening of the material [13]. However, K atoms are relatively challenging to use for STM-based studies, as they easily diffuse on the surface of

BP and can be laterally perturbed by the tip-generated electric field.

Here, we explore the influence of a single donor, derived from an individual Cu atom, on the bistable valency of an isolated Co atom on BP. Using first principle calculations based on density functional theory (DFT), we find that individual Cu atoms residing in various binding sites as well as hydrogenated species can be modeled as individual positively charged ions on the surface. Based on these findings, we measured the changes in measured ionization energy of one of the orbital states of individual Co atoms, in proximity of a positively charged Cu donor, using STM/STS with atomic manipulation. Considering the various sources of electrostatic interactions, we show that the changes in ionization energy originate from local band bending arising from a screened Coulomb interaction of the Cu donor. We additionally observe a strong change in the orbital state-dependent lifetime of the ionized Co atom, in the stochastic limit, depending on the separation between a Co atom and Cu donor. This strong orbital state dependence in the measured lifetimes results from the interplay between the influence of the Cu gating field and the different dielectric screening of the two orbital states. We further find, from first principles calculations based on DFT, that each valency exhibits a significant electric dipole moment oriented perpendicular to the surface, leading to a substantially different response to the local electric field generated by the STM tip.

Figure 1(a) illustrates an STM image of a cleaved BP surface after deposition of Co and Cu atoms [14–27]. In agreement with previous experiments [28], intrinsic vacancies are identified as elongated dumbbell-shaped protrusions. An individual Co atom preferentially adsorbs onto a top site, and its charge density can be identified as a
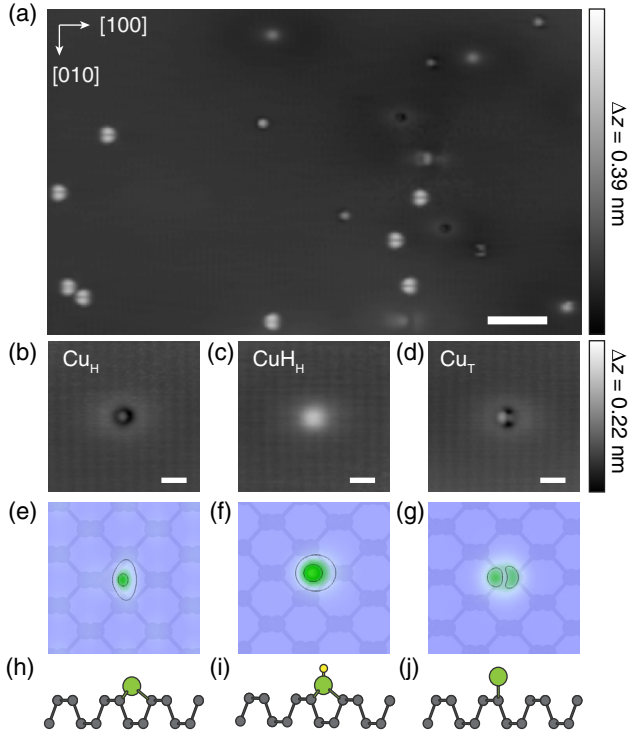
FIG. 1. (a) STM image of individual Co and Cu atoms on the surface of BP. ($V_S = -400$ mV, $I_t = 20$ pA, scalebar = 5 nm). (b)–(d) STM images of the charge density of three Cu species: (b) Cu residing in a hollow site (Cu_H), (c) hydrogenated Cu residing in a hollow site (CuH_H) and (d) Cu residing on a top site (Cu_T). ($V_S = -400$ mV, $I_t = 60$ pA, scalebar = 1 nm). (e)–(g) *Ab initio* calculations of the relaxed charge density of (e) a Cu_H atom, (f) CuH_H, and (g) a Cu_T atom. (h)–(j) Schematics of the relaxed atomic adsorption geometries of (h) Cu_H, (i) CuH_H, and (j) Cu_T.

bilobed, butterflylike shape. The Co atom can be manipulated into a hollow site, using the STM tip [3]. In constant-current STM imaging, Co atoms residing in a hollow site can exhibit two different charge densities (Co_{high} and Co_{low}). These two unique charge densities result from the bistable valency of the Co atom [3], and can be reversibly switched with a voltage pulse. Cu atoms can be differentiated from Co atoms due to their distinguishable charge densities in constant-current imaging. Three different Cu species were observed, all characterized by an ellipse-shaped outer depression whereas the internal pattern is distinct between all three species [Figs. 1(b)–1(d) and the Supplemental Material [14]].

In order to quantify the electronic properties of each Cu species and relate this to the experimental observations, we performed DFT calculations for a Cu atom on the BP surface [14]. We calculated the band structure of Cu atoms residing on a top site (Cu_T) and in a hollow site (Cu_H) on BP, as well as of hydrogenated Cu in the hollow site (CuH_H) (Supplemental Material [14], Fig. S3). In case of Cu_H and CuH_H, the system is nonmagnetic, whereas a

small magnetic moment of $\sim 0.5~\mu_B$ appears for Cu_T. We also calculated the spatial distribution of the charge densities projected on the valence states of BP [Figs. 1(e)–1(g)], which can be directly associated with the STM images [Figs. 1(b)–1(d)]. Based on these calculations, we conclude that the experimentally observed species in Figs. 1(b) and 1(d) are the hollow and top site, respectively. We also confirm that the charge density observed in Fig. 1(c) coincides with CuH_H. From DFT calculations it follows that $Cu_H/CuH_H/Cu_T$ species donate 0.7/0.12/0.24 electrons to the BP substrate, respectively. The electrons are mostly donated from the $4s$ shell of Cu, whereas the $3d$ shell remains fully occupied. These calculations are consistent with experimental observations of n doping at higher Cu coverages (Supplemental Material [14], Fig. S2). Therefore, we consider all Cu species as donors in the subsequent discussion, in line with previous literature [29–32]. In the following experiments, a relatively low areal density of $n_{Cu} = 0.165 \times 10^{12}$ cm^{-2} was used to ensure minimal band shifts in the BP (<8 meV).

In order to probe the influence of Cu donors on the bistable valency of individual Co atoms, we first studied the response of the Co_{low} atom charging peak as a function of distance (r) from a single, isolated Cu atom. As shown in Ref. [3], Co impurity states near E_F can be pulled above E_F, via tip-induced band bending [33–35]. This leads to a peak in STS near $V_S = 370$ mV, which depends on the tip and tunneling conditions. We observed that this charging peak shifts to higher energy [$\Delta V_r = 118$ mV, defined with respect to the peak energy of an isolated atom, $\Delta V_r = V(r) - V(r > 10$ nm)] when the Co atom is near CuH_H ($r = 3.8$ nm) (Fig. 2).

In order to quantify this influence of the Cu donor, we measured the charging peak shift ΔV_r at various values of r and for the three different Cu species (Fig. 3 and Supplemental Material [14], Fig. S4). The studied Co-Cu pairs were created utilizing atomic manipulation of Co atoms. At distances of approximately $r > 10$ nm, there is no shift of the ionization energy, i.e., ΔV_r is negligible. At smaller distances, we observe a monotonously increasing, strongly nonlinear trend in ΔV_r. The observed charging peak shift corresponds to a shift of the Co energy level that is being swept through E_F, as depicted in the inset of Fig. 3. This can stem from three effects: (i) Local band bending (i.e., gating of the conduction band) induced by the positively charged Cu atom. In the simple limit that the Cu atom can be approximated as a point charge, the generated electric field is not fully screened. Therefore, we can approximate this band bending by a Yukawa potential due to the screening from the substrate: $V_{Cu} = (g/r)e^{(-r/r_c)}$. Here, g is a scaling constant and r_c the effective screening length. (ii) Changes in the tip-induced band-bending (TIBB), that additionally contribute when another mechanism [e.g., point (i)] shifts the overall charging peak onset. We can assume that the TIBB scales linearly with applied bias in
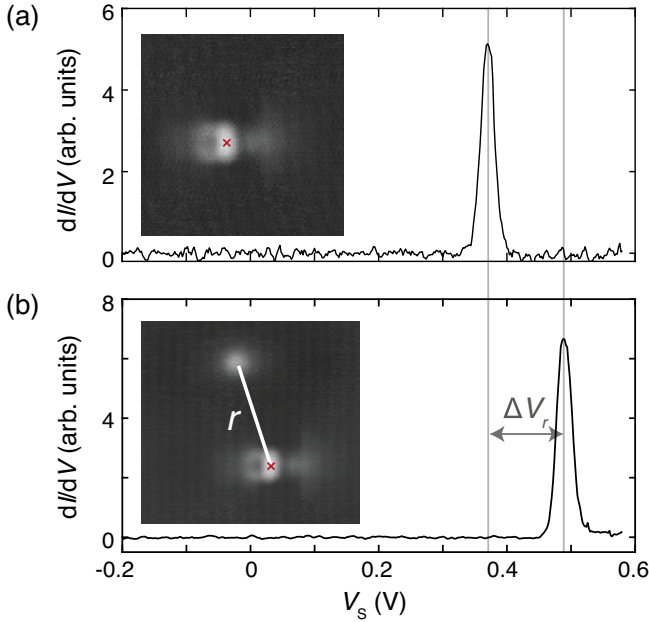
FIG. 2. (a) dI/dV spectrum taken on an isolated Co_{low} atom (distance to nearest Cu species $r > 10$ nm). Inset: STM image of the isolated Co_{low} atom ($V_S = -400$ mV, $I_t = 60$ pA). (b) dI/dV spectrum taken on a Co_{low} atom in the vicinity of CuH_H (distance $r = 3.8$ nm). The shift of the ionization peak with respect to the isolated atom is indicated by ΔV_r and equals 118 mV. Inset: STM image of the Co_{low}-CuH_H pair. The red X in both insets (a)–(b) mark the locations where the dI/dV spectra were taken. ($V_S = -400$ mV, $I_t = 60$ pA).

FIG. 3. Shift of the ionization peak energy ΔV_r of single Co_{low} atoms as a function of distance to a Cu species r. The shift is defined with respect to the peak energy of an isolated atom: $\Delta V_r = V(r) - V(r > 10 \text{ nm})$. Different colors represent different microtips. The solid line is a fit to the Yukawa potential, with parameters $g = 4.88$; $r_c = 1.93$ nm. In the inset, a schematic band diagram shows downward band bending of the Co energy level (which is pulled through E_F by TIBB) in the presence of a Cu species.

the relevant energy range (see, for example, Ref. [36]). Such linear changes cannot explain the nonlinear behavior observed in Fig. 3, but it may change the scaling constant of the Yukawa potential. Furthermore, TIBB is strongly tip dependent. To account for these differences, we use ΔV_r instead of V_S and the measurement was performed using different tips. As we show in Fig. 3, ΔV_r is roughly the same independent of the given tip. Therefore, we expect the variations in TIBB in the applied voltage range to be negligible. (iii) DFT calculations reveal that the Co atom has an electric dipole moment ($\boldsymbol{p}_i$), where i labels the orbital state (see Supplemental Material [14], Fig. S6). This calculated moment is oriented perpendicular to the surface. In the simplest limit, the subsequent change in energy equals $\Delta V_{\text{dipole}} = \boldsymbol{p} \cdot \boldsymbol{E}$. The electric field of the tip can lead to a strong change in this energy, but this does not depend on the distance of the Cu atom (r). The electric field of the tip does depend on the tip-sample separation and the bias V_S. The tip-sample separation is constant in the experiments, but the bias is not. Like in (ii), the consequential changes to the experimentally probed ΔV_r are expected to be linear and cannot explain the nonlinearity observed. As we detail in the Supplemental Material [14], this may explain why there are differences in the overall asymmetry as a function of applied voltage (as reported in our original paper [3]), compared to changing r. In the same way,

the electric field of a Cu atom can couple to the dipole moment of the Co atom. However, since the field and dipole are nearly orthogonal, we can neglect this effect. Therefore, the only nonlinear factor governing the shift of the charging peak energy level is point (i), the band bending induced by the presence of a Cu donor. Using this information, we fit the data in Fig. 3 with a Yukawa potential. The extracted effective screening length equals $r_c = 1.93$ nm.

To understand the influence of a local electric field on orbital memory, we studied the influence of a Cu-based donor on the stochastic noise of a nearby Co atom as a function of r (Fig. 4). By applying voltages typically above $V_S > 400$ mV, isolated Co atoms exhibit telegraph noise resulting from stochastic switching between the bistable valencies: Co_{high} and Co_{low} [Fig. 4(a)] [3]. We subsequently measured the telegraph noise of a Co atom, within the proximity of a Cu species. We measured the telegraph noise until we approach steady state (typically ~800 switching events), in order to be able to extract the state dependent lifetime (τ_{high} and τ_{low}), as done in Refs. [3,37]. We extracted τ_{high} and τ_{low} for multiple tips and atoms, with varying values of r [Figs. 4(b)–4(c)] at two sample biases: $V_S = 500$ and 550 mV (more biases are shown in Supplemental Material [14], Fig. S5). As in Fig. 3, the results in Figs. 4(b)–4(c) include Co-Cu_T, Co-Cu_H, and Co-CuH_H pairs in various orientations and directions. The most striking feature is that the lifetime of the Co_{high} state

(τ_{high}) is dramatically decreased by the proximity of the Cu donor, whereas the Co_{low} state is only weakly perturbed in comparison. At $V_S = 500$ mV, lifetime τ_{high} decreases from approximately 170 to 30 ms for decreasing r from ~16 to 4 nm and at $V_S = 550$ mV, τ_{high} decreases more than an order of magnitude, from roughly 70 to 5 ms. We propose that the dependence of τ_{high}/τ_{low} on r, is derived purely from the gating effects of the Cu—a local shifting of the bands. The reason why τ_{low} is not affected in proximity to Cu, is that the effective screening length of the given orbital state is roughly 2 nm (derived from the Yukawa fit in Fig. 3), thus the Cu is only a weak perturbation at $r > 4$ nm. As we know from Ref. [3], the dielectric screening of the Co_{high} state from the substrate is weaker, meaning the effective screening length should increase. Therefore, the onset of changes to τ_{high} should occur at larger values of r compared to τ_{low}.

It is interesting to compare the effect of the electric field of a Cu donor to the effect of the tip electric field on the stochastic switching of a Co atom. A higher bias V_S presents a larger net electric field from the tip similar to Cu, and if the effect of a higher tip field is comparable to that of the field generated by a Cu atom, we should observe similar trends in both the mean lifetime and asymmetry of

the orbital states. In the case of a higher applied bias voltage for an isolated atom without a Cu atom in the vicinity, we most prominently observe a strong decrease in the mean lifetime of the Co atom [3], whereas the influence of the gating field of Cu is strongly state selective, mainly influencing the lifetime of one orbital state (Co_{high}). This illustrates that there are different mechanisms at play between these two effects. As the tip field is most likely aligned with the dipole moment of Co, we conclude that the mechanism at play here likely results from dipolar coupling (i.e., a Stark-like effect). In this picture, a higher applied bias would strongly increase the energy in the system and mimic an effective temperature. In contrast, the Cu donor strongly influences the local band bending and therefore locally gates the orbital states of the individual Co atom.

In conclusion, we demonstrated the effect of a controlled electric field generated by an individual Cu donor on the atomic orbital memory of Co on BP. Using both STM/STS and DFT calculations, we quantified the distance-dependent influence of individual Cu donors on the ionization energy of Co, as well as on the state-dependent lifetime in the stochastic limit. The monotonous increase in the charging energy of Co_{low} with decreasing r maps the downward band bending associated with the single
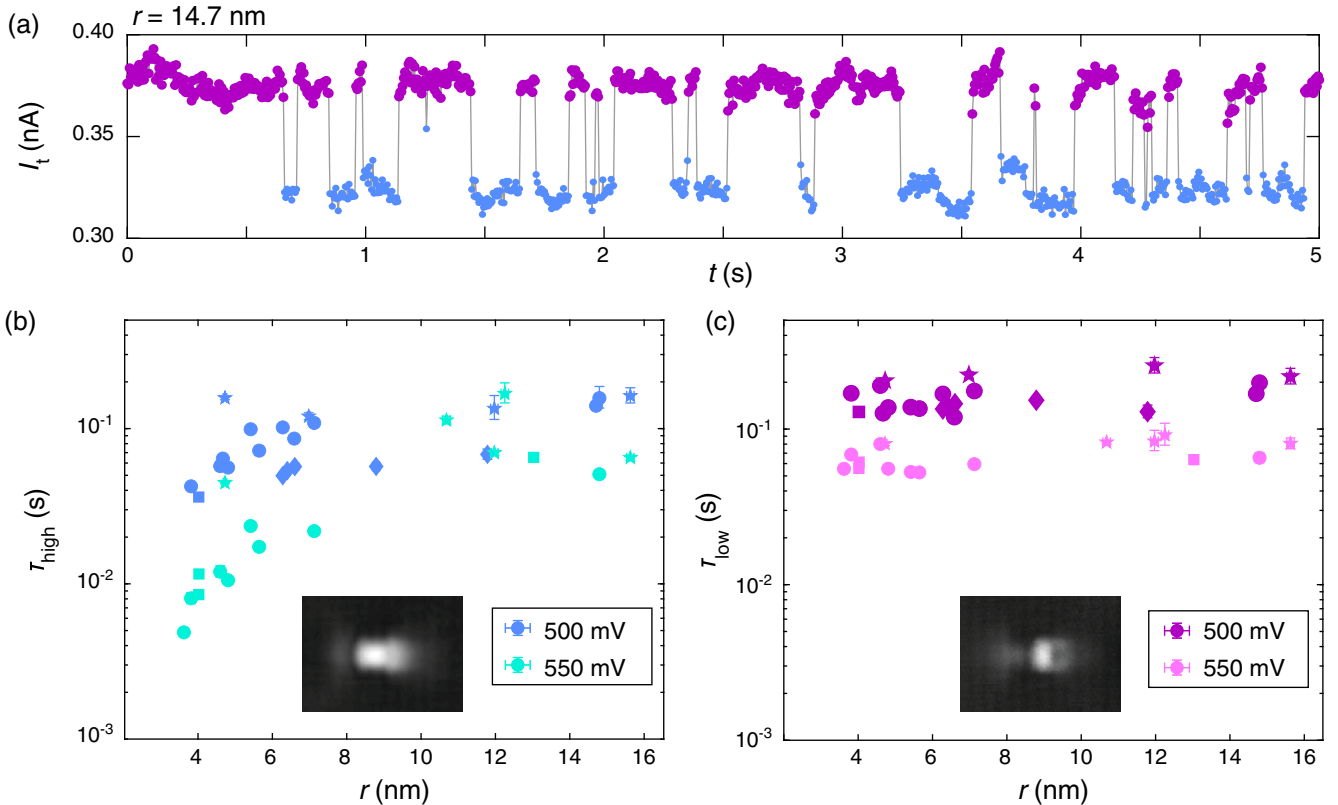
FIG. 4. (a) Two-state telegraph noise signal of an isolated Co atom (nearest Cu donor at $r = 14.7$ nm), with Co_{low} in purple and Co_{high} in blue. (b)–(c) State lifetime τ of (b) Co_{high} and (c) Co_{low} as a function of r. Different symbols represent different microtips and different colors represent different biases (500 and 550 mV). In the insets, STM images of the corresponding states Co_{high} and Co_{low} are displayed ($V_S = -400$ mV, $I_t = 60$ pA).

Cu atoms and follows the characteristic behavior for a screened Coulomb interaction. We also find that the proximity to a local donor strongly influences the lifetime of the Co_{high} state in the stochastic limit, whereas there is no influence on the lifetime of the Co_{low} state. We attribute this to a gating effect of the Cu donor, impacting the valencies differently because of their distinct screening from the substrate. Notably, we detected no difference in the effect of the different Cu species on the ionization energy or stochastic behavior of Co. Furthermore, DFT calculations provided evidence of a state-dependent electric dipole moment for Co_{low} and Co_{high}, which can explain the response of the lifetimes as a function of bias V_S by a dipolar coupling between the Co atom and the tip electric field. Our findings illustrate how the state favorability of an atomic orbital memory, i.e., the energy landscape, can be tuned by an external electric field, analogous to a magnetic field in a spin-based memory. It remains to be seen how the spin states and crystal field are locally affected by the presence of the electric field.

[1] T. O. Wehling, A. I. Lichtenstein, and M. I. Katsnelson, Phys. Rev. B **84**, 235110 (2011).

[2] A. N. Rudenko, F. J. Keil, M. I. Katsnelson, and A. I. Lichtenstein, Phys. Rev. B **86**, 075422 (2012).

[3] B. Kiraly, A. N. Rudenko, W. M. J. van Weerdenburg, D. Wegner, M. I. Katsnelson, and A. A. Khajetoorians, Nat. Commun. **9**, 3904 (2018).

[4] A. Kolmus, M. I. Katsnelson, A. A. Khajetoorians, and H. J. Kappen, New J. Phys. **22**, 023038 (2020).

[5] U. Kamber, A. Bergman, A. Eich, D. Iuşan, M. Steinbrecher, N. Hauptmann, L. Nordström, M. I. Katsnelson, D. Wegner, O. Eriksson, and A. A. Khajetoorians, Science **368**, eaay6757 (2020).

[6] B. Kiraly, E. J. Knol, W. M. J. van Weerdenburg, H. J. Kappen, and A. A. Khajetoorians, Nat. Nanotechnol. **16**, 414 (2021).

[7] F. Donati, S. Rusponi, S. Stepanow, C. Wäckerlin, A. Singha, L. Persichetti, R. Baltic, K. Diller, F. Patthey, E. Fernandes, J. Dreiser, Ž. Šljivančanin, K. Kummer, C. Nistor, P. Gambardella, and H. Brune, Science **352**, 318 (2016).

[8] F. E. Kalff, M. P. Rebergen, E. Fahrenfort, J. Girovsky, R. Toskovic, J. L. Lado, J. Fernández-Rossier, and A. F. Otte, Nat. Nanotechnol. **11**, 926 (2016).

[9] F. D. Natterer, K. Yang, W. Paul, P. Willke, T. Choi, T. Greber, A. J. Heinrich, and C. P. Lutz, Nature (London) **543**, 226 (2017).

[10] J. Kim, S. S. Baik, S. H. Ryu, Y. Sohn, S. Park, B.-G. Park, J. Denlinger, Y. Yi, H. J. Choi, and K. S. Kim, Science **349**, 723 (2015).

[11] S.-W. Kim, H. Jung, H.-J. Kim, J.-H. Choi, S.-H. Wei, and J.-H. Cho, Phys. Rev. B **96**, 075416 (2017).

[12] C. Han, Z. Hu, L. C. Gomes, Y. Bao, A. Carvalho, S. J. R. Tan, B. Lei, D. Xiang, J. Wu, D. Qi, L. Wang, F. Huo, W. Huang, K. P. Loh, and W. Chen, Nano Lett. **17**, 4122 (2017).

[13] B. Kiraly, E. J. Knol, K. Volckaert, D. Biswas, A. N. Rudenko, D. A. Prishchenko, V. G. Mazurenko, M. I. Katsnelson, P. Hofmann, D. Wegner, and A. A. Khajetoorians, Phys. Rev. Lett. **123**, 216403 (2019).

[14] See Supplemental Material at http://link.aps.org/supplemental/10.1103/PhysRevLett.128.106801 for methods and detailed information on: Cu species, Cu doping of BP, the ionization energy of Co atoms, bias dependence of stochastic switching of Co, and calculations of the electric dipole moment of Co. This includes Refs. [15–27].

[15] P. E. Blöchl, Phys. Rev. B **50**, 17953 (1994).

[16] G. Kresse and J. Furthmüller, Phys. Rev. B **54**, 11169 (1996).

[17] G. Kresse and D. Joubert, Phys. Rev. B **59**, 1758 (1999).

[18] J. P. Perdew, K. Burke, and M. Ernzerhof, Phys. Rev. Lett. **77**, 3865 (1996).

[19] A. Brown and S. Rundqvist, Acta Crystallogr. **19**, 684 (1965).

[20] N. Marzari, A. A. Mostofi, J. R. Yates, I. Souza, and D. Vanderbilt, Rev. Mod. Phys. **84**, 1419 (2012).

[21] A. A. Mostofi, J. R. Yates, Y.-S. Lee, I. Souza, D. Vanderbilt, and N. Marzari, Comput. Phys. Commun. **178**, 685 (2008).

[22] J. Tersoff and D. R. Hamann, Phys. Rev. B **31**, 805 (1985).

[23] A. Zhao, Q. Li, L. Chen, H. Xiang, W. Wang, S. Pan, B. Wang, X. Xiao, J. Yang, J. G. Hou, and Q. Zhu, Science **309**, 1542 (2005).

[24] N. Baadji, S. Kuck, J. Brede, G. Hoffmann, R. Wiesendanger, and S. Sanvito, Phys. Rev. B **82**, 115447 (2010).

[25] B. W. Heinrich, G. Ahmadi, V. L. Müller, L. Braun, J. I. Pascual, and K. J. Franke, Nano Lett. **13**, 4840 (2013).

[26] A. A. Khajetoorians, T. Schlenk, B. Schweflinghaus, M. dos Santos Dias, M. Steinbrecher, M. Bouhassoune, S. Lounis, J. Wiebe, and R. Wiesendanger, Phys. Rev. Lett. **111**, 157204 (2013).

[27] V. C. Zoldan, R. Faccio, and A. A. Pasa, Sci. Rep. **5**, 8350 (2015).

[28] B. Kiraly, N. Hauptmann, A. N. Rudenko, M. I. Katsnelson, and A. A. Khajetoorians, Nano Lett. **17**, 3607 (2017).

[29] S. P. Koenig, R. A. Doganov, L. Seixas, A. Carvalho, J. Y. Tan, K. Watanabe, T. Taniguchi, N. Yakovlev,

A. H. Castro Neto, and B. Özyilmaz, Nano Lett. **16**, 2145 (2016).

[30] S. W. Lee, L. Qiu, J. C. Yoon, Y. Kim, D. Li, I. Oh, G.-H. Lee, J.-W. Yoo, H.-J. Shin, F. Ding, and Z. Lee, Nano Lett. **21**, 6336 (2021).

[31] Z. Lin, J. Wang, X. Guo, J. Chen, C. Xu, M. Liu, B. Liu, Y. Zhu, and Y. Chai, InfoMat. **1**, 242 (2019).

[32] Y. Zheng, H. Yang, C. Han, and H. Y. Mao, Adv. Mater. Interfaces **7**, 2000701 (2020).

[33] R. M. Feenstra, J. Vac. Sci. Technol. B **21**, 2080 (2003).

[34] F. Marczinowski, J. Wiebe, F. Meier, K. Hashimoto, and R. Wiesendanger, Phys. Rev. B **77**, 115318 (2008).

[35] K. Teichmann, M. Wenderoth, S. Loth, R. G. Ulbrich, J. K. Garleff, A. P. Wijnheijmer, and P. M. Koenraad, Phys. Rev. Lett. **101**, 076103 (2008).

[36] G. J. de Raad, D. M. Bruls, P. M. Koenraad, and J. H. Wolter, Phys. Rev. B **66**, 195306 (2002).

[37] A. A. Khajetoorians, B. Baxevanis, C. Hübner, T. Schlenk, S. Krause, T. O. Wehling, S. Lounis, A. Lichtenstein, D. Pfannkuche, J. Wiebe, and R. Wiesendanger, Science **339**, 55 (2013).